

# Light refraction in the earth's atmosphere I. Inferior mirages: analytic solution of ray paths

C. Alejandro Paola

*Facultad de Ciencias Astronómicas y Geofísicas, Univesidad Nacional de La Plata,  
Paseo del Bosque s/n, La Plata, Buenos Aires, Argentina;  
Tel: (54) 221 4236593; Fax: (54) 221 4236591;  
Universidad Tecnológica Nacional, Facultad Regional La Plata,  
Avenida 60 esquina 124 s/n, La Plata, Buenos Aires, Argentina.  
Tel: (54) 221 4124300.  
e-mail: apaola@fcaglp.unlp.edu.ar*

A. Cruzado

*Facultad de Ciencias Astronómicas y Geofísicas, Univesidad Nacional de La Plata,  
Paseo del Bosque s/n, La Plata, Buenos Aires, Argentina;  
Instituto de Astrofísica de La Plata,  
Paseo del Bosque s/n, 1900 La Plata, Buenos Aires, Argentina.  
Tel: (54) 221 4236593; Fax: (54) 221 4236591.  
e-mail: acruzado@fcaglp.unlp.edu.ar; alicehaiadjamian@yahoo.com.ar*

F. M. Carrasco Galleguillos

*Facultad de Ciencias Astronómicas y Geofísicas, Univesidad Nacional de La Plata,  
Paseo del Bosque s/n, La Plata, Buenos Aires, Argentina;  
Oficina de Riesgo Agropecuario, Ministerio de Agricultura, Ganadería y Pesca,  
Av. Paseo Colón 922, piso 2, oficinas 233 y 234, Ciudad Autónoma de Buenos Aires, Buenos Aires, Argentina.  
Tel: (54) 221 4236593; Fax: (54) 221 4236591.  
e-mail: felix.marcial@gmail.com*

Received 17 November 2021; accepted 10 January 2022

We aim to reach an analytic expression that describes the path of light rays through the Earth's atmosphere in the particular situation in which an inferior mirage is occurring. To achieve our goal, we assume an exponential refractive index profile close to the ground, as suggested by empirical and theoretical studies on the state of air when an inferior mirage is taking place. We consider a parallel-plane atmosphere and assume that the laws of geometric optics apply. Since Fermat's principle holds, we solve the Euler's equation and, from the solution we obtain an analytic expression that describes the ray paths in a plane perpendicular to the ground. Given that we focus on the particular case of inferior mirages, we were able to find a very simple and easy-to-use expression to describe the ray paths, allowing us to extract additional valuable information with minimal computational effort. We take advantage of it to impose a limit to the thickness of the air layer next to the ground where appropriate conditions exist to bend the rays upwards, and produce an inferior mirage.

*Keywords:* Planetary atmospheres; light refraction; inferior mirages; analytic expression.

DOI: <https://doi.org/10.31349/RevMexFis.68.041301>

## 1. Introduction

This is the first of a series of works in which we intend to deal with different optical phenomena taking place in planetary atmospheres. We will begin by addressing the study of some phenomena related to light refraction that are known to occur in the Earth's atmosphere. The refraction of light in the Earth's atmosphere is a topic of great interest to astronomers, geophysicists, and meteorologists. Refraction is an unavoidable issue whenever we are dealing with the propagation of radiation through the terrestrial atmosphere, in relation to the image formation of either astronomical or terrestrial sources, or in relation to radio communication and radar systems. At the first works we will focus on image formation.

Regarding the study of refraction for astronomical purposes, more or less complete treatments appear in general or spherical astronomy textbooks as old as Danjon (1959) [1]. Mahan (1962) [2], Garfinkel (1967) [3], and Yatsenko (1995) [4], just to name a few, have published on astronomical refraction. Many publications proposing new approaches and formulas for the calculation of refraction, in particular near the horizon, are found in the literature. A very valuable contribution has been made by Young (2006) [5], who focuses on the physics of refraction beyond formulas and numerical calculations. Many authors have, also, studied in detail the influence of refraction in observations of the sun (Corbard *et al.*, 2019 [6]).

In the present paper we deal with image formation of terrestrial sources, particularly, inferior mirages. An inferior mirage is an atmospheric optical phenomenon often seen on summer days on highways and deserts. The soil surface is heated by the sun causing a strong temperature gradient in the air layers closest to the ground.

Several articles referring to the light ray paths through refractive media are found in the literature. Evans and Rosenquist (1986) [7] and Evans (1990) [8] presented an original formulation of the theory of light rays in variable refractive index media. From the variational principle, they derived a differential equation for a ray of light similar to Newton's law of motion for a particle in a conservative force field. In the first of these papers they even solved this equation for the particular case of inferior mirages assuming a linearly varying refractive index. Nener *et al.* (2003) [9] found, working in spherical coordinates, an expression describing the ray paths with exact solution for linear and quadratic refractive index profiles. In a later article (Fowkes & Nener, 2005 [10]), they adopt a refractive index that varies exponentially near the ground and linearly higher up, finding thus two solutions to describe the paths of light rays, the inner and the outer solution.

Many articles based on the ray tracing technique have, also, been published. With this method, so widely used in computer graphics, they created algorithms that allowed them to simulate different optical phenomena (Berger *et al.*, 1990 [11], Musgrave, 1990 [12], Stam and Languenou, 1996 [13], Gutierrez *et al.*, 2006 [14]).

In this series, we aim to individually analyze each phenomenon related to the refraction of light in the Earth's atmosphere. This will allow us to make the appropriate considerations in each particular case and thus achieve simpler analytic expressions. Our objective in the present work is to find such an expression describing the path followed by light when an inferior mirage is taking place.

To develop our ideas, we consider a plane-parallel atmosphere assuming that in each layer all the physical parameters characterizing it remain constant. All investigations related to atmospheric conditions that give rise to inferior mirages show that the required temperature inversion occurs very close to the ground. Personal experiences verify it. Only our feet are able to feel the high temperatures of a surface heated by the sun's rays. The upward heat transport that takes place creates a temperature profile characterized by a sharp 10 – 20°C drop in a few centimeters of air. When going from a sitting to a standing position, we are not able to notice such a drop in temperature. The departure of the air refractive index from its normal conditions, that will cause the light rays to bend upwards, occurs, then, very close to the ground. The paths of light rays from objects in our environment can be considered straight lines for most of their travel. The distances traveled by light within the layers of air that curve it upward are too short to take into account the earth sphericity. We also assume that the geometrical optics laws apply. A detailed analysis of the validity ranges of this assumption are found

in Born & Wolf (1959) [15] and Jackson (1975) [16]. Since light travels an optical path that is stationary with respect to variations of that path, the Fermat's principle is applied in order to compute the path of light.

Our approach to the problem will be correct as long as we are dealing with refractive media in which the refractive index,  $n$ , only varies with one coordinate, and the particular solution we found will remain valid provided that the refractive index varies with that coordinate in the exponential way that we propose. The refractive index profile we propose is not, however, a limitation, if what we want to study are inferior mirages. As we will see later, the profile we have adopted for  $n$  is the one suggested by both theoretical and experimental research on the subject.

We organize this paper as follows: In Sec. 2 we address the issue of heat transport in the microlayer. In Sec. 3 we study the paths of light rays, dealing with mathematical development that leads us to find the analytic expression we are looking for in Sec. 3.1. Then, a description of the light ray paths and an analysis of the expression obtained is presented in Sec. 3.2. Finally, in Sec. 4 we briefly summarize our results and reach our conclusions.

## 2. Heat transport

In this section, we aim to find a feasible refractive index profile under the conditions in which mirages occur. Several authors argue that the appropriate atmospheric conditions to produce mirages occur very close to the ground (Stull, 1988 [17], Stam and Languenou, 1996 [13]). Solar radiation heats the surface of the road raising its temperature well above the air temperature, which causes upward heat transport by molecular and turbulent processes through the microlayer. We do not intend to work out a detailed profile of the parameters that describe the atmosphere, but just to find the way in which, under given conditions, the air temperature in the microlayer decreases with height. A rigorous treatment of the energy balance taking into account downwards and upwards radiation is not justified, neither a detailed approach to convection. The way we have dealt the heat transport through the microlayer will be explained in the following paragraphs.

We write the heat flux across the microlayer,  $Q$ , as the sum of two terms

$$Q = Q_c + Q_t, \quad (1)$$

being  $Q_c$  and  $Q_t$  the heat transported by molecular and turbulent processes, respectively.

By setting the origin of the Cartesian coordinate system on the ground and the y-coordinate axis perpendicular to it, the heat transported by conduction can be written as

$$Q_c = -\kappa \frac{\delta T}{\delta y}, \quad (2)$$

being  $\kappa$  the thermal conductivity of air. To take into account the temperature dependence of  $\kappa$  we use the expression of Kannuliik and Carman (1951) [18],

$$\kappa = 5.75 \times 10^{-5} (1 + 0.00317T - 0.0000021T^2), \quad (3)$$

where  $[T] = ^\circ\text{C}$  and  $[\kappa] = \text{Cal}/^\circ\text{C cm s}$ .

Regarding convective transport, we made the following assumptions: i) we only took into account turbulent flux, since the vertical advective flux is negligible compared to the turbulent one (Stull, 1988 [17]) and we are only interested in upward heat flux, and ii) under the constraint of total heat flux conservation, we express turbulent flux as a fraction  $f$  of the molecular one, taking into account that conduction dominates very close to the ground, decreasing with the height as turbulence increases. Therefore Eq. (1) can be written as

$$Q\delta y = -(1 + f)\kappa\delta T. \quad (4)$$

Taking into account the  $\kappa$  dependence on  $T$  given by Eq. (3), we integrate both members of the expression (4) and iteratively solve it to find the variation of temperature with height from the ground. The total heat flux,  $Q$ , and the ground temperature,  $T_0$ , are parameters adopted at the beginning. Although  $Q$  and  $T_0$  are not actually independent parameters of each other, they are not unambiguously related; their relationship depends on the kind of surface. Taking them as unrelated parameters allows us to observe the influence of each one on the results, not affecting our conclusions at all. We have done calculations by making  $f$  vary with height in different ways. The way  $f$  varies with height determines the height from the ground at which the molecular and turbulent processes are of the same magnitude. That height in turn determines how quickly the temperature drops and, thus, the  $T_f$  environment temperature reached away from the ground. Working in this way, we achieve results like those shown in Figs. 1, 2 and 3.

In Fig. 1, where the heat transported by molecular and turbulent processes as functions of height are drawn, we have managed to obtain a diagram similar to the one shown in Fig. 7.1b) of Stull (1988) [17] assuming  $Q = 260 \text{ W/m}^2$

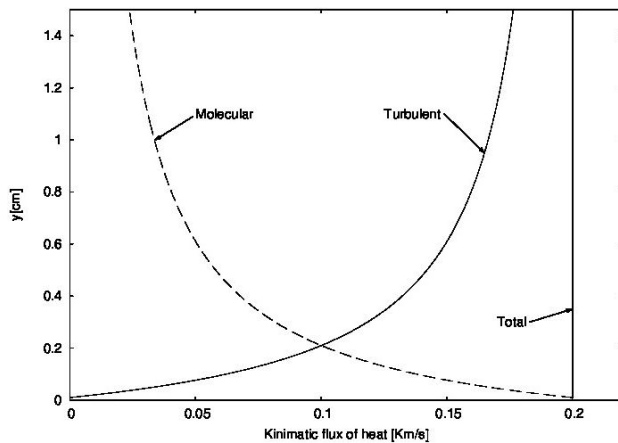


FIGURE 1. Heat transport. A solid line shows the turbulent heat flux, and a dashed line shows the molecular heat one. The total flux, equivalent to  $200 \text{ W/m}^2$ , is also indicated.

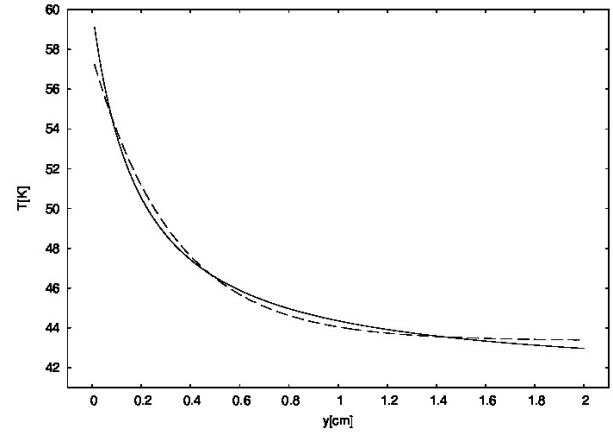


FIGURE 2. Temperature profile. A solid line shows the atmospheric temperature profile near the ground obtained from our calculations, and a dashed line shows the fitted exponential function.

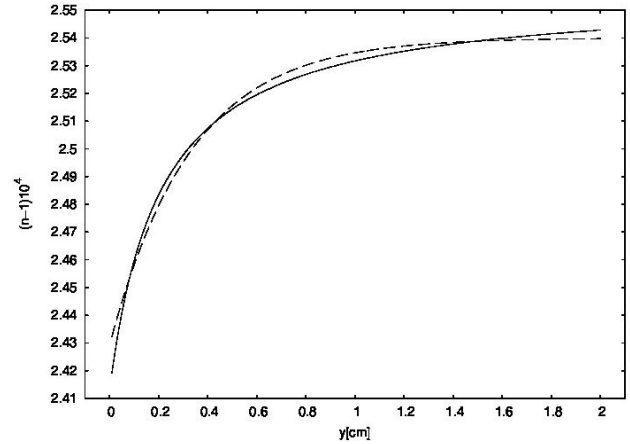


FIGURE 3. Refractive index profile. A solid line shows the refractive index profile of the air close to the ground gotten from our calculations, and a dashed line shows the fitted exponential function.

(equivalent to a kinematic heat flux  $Q/\rho C_p = 0.2 \text{ Km/s}$  as it is expressed by Stull, 1988 [17]).

Although we are not particularly interested in the course of the heat fluxes through the microlayer, this figure is useful just to check that the way we have modeled the heat transport mechanisms makes things go reasonably well. As can be seen in the figure, the turbulent heat transport takes on the same importance as the molecular one at 2 mm from the ground.

Assuming  $T_0 = 60^\circ\text{C}$ , the temperature profile through the microlayer, displayed with solid line in Fig. 2, is obtained.

Its sharp drop in the lowest millimeters of air is apparent. It is also clear that the temperature as a function of height can be adjusted with an exponential function like

$$T = T_f(1 + \epsilon \exp(-y/h_0)), \quad (5)$$

where  $\epsilon = T_0/T_f - 1$  is obtained by setting  $y = 0$  in Eq. (6), and  $h_0$  is a positive constant to be determined in each par-

ticular case. So, in terms of  $T_0$  and  $T_f$  the temperature as a function of height can be written as

$$T = T_f + (T_0 - T_f) \exp(-y/h_0). \quad (6)$$

The dashed curve displayed in Fig. 2 is obtained for  $h_0 = 0.33$  cm. Such a sudden exponential drop in temperature very close to the ground in the context of mirages sighting has already been argued by several authors (Stull, 1988 [17], Stam and Langenou, 1996 [13]).

To obtain  $n$  as a function of height we take into account that it can be written so that

$$n - 1 = \delta \times 10^{-6} D, \quad (7)$$

where  $\delta$  is the refractivity for atmospheric pressure  $P = 76$  cmHg and temperature  $t = 0^\circ\text{C}$ , and  $D$  is the pressure and temperature correction factor. Both,  $\delta$  and  $D$ , are dimensionless parameters.

To take into account the  $\delta$  dependence on the wavelength of light we have used the Ciddor (1996) [19] formula

$$n - 1 = \frac{0.05792105}{238.0185 - \lambda^{-2}} + \frac{0.00167917}{57.362 - \lambda^{-2}}, \quad (8)$$

given for  $t = 15^\circ\text{C}$ ,  $P = 76$  cmHg, and 0% humidity, with  $\lambda$  in microns.

The factor  $D$  can be written as

$$D = \frac{P}{76} \frac{273}{(t + 273)}, \quad (9)$$

with  $P$  in cmHg and  $t$  in  $^\circ\text{C}$ .

Assuming  $t = 15^\circ\text{C}$  and  $P = 76$  cmHg for the calculation of  $D$  in Eq. (7) and equating to Eq. (8),  $\delta$  can be calculated for any  $\lambda$  value as

$$\delta = \left[ \frac{0.05792105}{238.0185 - \lambda^{-2}} + \frac{0.00167917}{57.362 - \lambda^{-2}} \right] \times \frac{(15 + 273)}{273} \times 10^6. \quad (10)$$

Then,  $n$  can be obtained for any  $t$  and  $P$  values from Eq. (7).

Then, by setting  $P = 76$  cmHg, and adopting the temperature profile shown in Fig. 2, we have obtained the refractive index as a function of height for  $\lambda = 0.5 \mu\text{m}$ , as shown with solid line in Fig. 3.

Given the  $n$  dependence on  $T$ , it is clear that the variation with the  $y$ -coordinate of the refractive index calculated for a temperature profile given by Eq. (6), can be fitted with a function like

$$n(y) = n_f \left[ 1 - \alpha \exp\left(-\frac{y}{\beta}\right) \right], \quad (11)$$

being  $n_f$  the  $n$  value far from the ground, where the temperature has reached the environment value  $T_f$ .  $\alpha$  and  $\beta$  are positive constants to be determined in each particular case,

that is, for each particular temperature profile. The best fit to our calculations is obtained by setting  $n_f = 1.00025$ ,  $\alpha = 1.10865 \times 10^{-5}$  and  $\beta = 0.33$  in Eq. (12), as we show with the dashed line in Fig. 3. Since  $\alpha = 1 - n_0/n_f$  is obtained by setting  $y = 0$  in Eq. (12), where  $n_0$  is the  $n$  value on the surface,  $n$  can be written in terms of  $n_0$  and  $n_f$  as

$$n(y) = n_f - (n_f - n_0) \exp\left(-\frac{y}{\beta}\right). \quad (12)$$

Then, we can also use the  $n_f$  and  $n_0$  values that we got from the calculations and only look for the  $\beta$  value that provides the best fit. The setting varies slightly.

We have made calculations varying  $Q$ ,  $T_0$  and the way  $f$  varies with height.  $Q$  was varied between  $200 \text{ W/m}^2$  and  $500 \text{ W/m}^2$  and  $T_0$  between  $40^\circ\text{C}$  and  $70^\circ\text{C}$ , as theoretical simulations and empirical measurements suggest (Garrat, 1991 [20], Heusinkveld, 2008 [21], Pfeiffer, 2021 [22]), although  $T_0$  higher than  $70^\circ\text{C}$  in unusual extreme conditions could occur. As for  $f$ , it is worth noting that the thicker the atmosphere layer in which molecular processes take place, the faster the temperature falls. Therefore, we have modeled  $f$  in such a way to achieve  $T_f$  values between  $40^\circ\text{C}$  and  $20^\circ\text{C}$ . We have limited ourselves to these  $T_f$  values since, except for very extreme conditions, the room temperature on days in which an inferior mirage could be observed will fluctuate between these values. For these  $T_f$  values, the height from the ground at which the molecular and turbulent processes are of the same magnitude has varied between 1 and 7 mm.

We have been able to verify that, for those parameter ranges,  $\alpha$  varies between  $1.1 \times 10^{-5}$  and  $4 \times 10^{-5}$ ,  $\beta$  ranges from 0.3 to 0.8 cm. Given the dependence on  $T$  of  $n$ , and taking into account the smallness of  $\delta \times 10^{-6}$ , it is clear that  $\beta$  and  $h_0$  will always be very similar.

### 3. Path of light rays.

#### 3.1. Search for an analytic expression.

Even though we are focused on the formation of inferior mirages, the following approach to the issue is suitable as long as we are dealing with a transparent medium in which the refractive index varies only with one coordinate. For the purpose of this paper, the assumption that the refractive index of the atmosphere varies only with distance to the ground is a very good approximation.

Given the symmetry of the problem, a two-dimensional analysis in the  $x - y$  plane restricted to positive  $x$  and  $y$  values is appropriate. Therefore, we can write the time interval it would take a ray of light to travel a differential path in the first quadrant of  $x - y$  plane as

$$dt = \frac{\sqrt{(dx)^2 + (dy)^2}}{v}, \quad (13)$$

or, in terms of the refractive index,

$$dt = \frac{n(y)}{c} \sqrt{1 + \left(\frac{dx}{dy}\right)^2} dy. \quad (14)$$

The time it takes the light to make its trip from  $y_0$  to  $y$  is obtained by means of the functional

$$T[f(y)] = \int_{y_0}^y \frac{n(y)}{c} \sqrt{1 + x'^2} dy, \quad (15)$$

where  $x' = dx/dy$ .

Since Fermat's principle predicts that light travels an optical path that is stationary with respect to variations of that path, the solution must satisfy the Euler's equation [16]

$$\frac{d}{dy} \left( \frac{\partial L}{\partial x'} \right) + \frac{\partial L}{\partial x} = 0, \quad (16)$$

with  $L(x, x', y) = \frac{n(y)}{c} \sqrt{1 + x'^2}$ .

Solving the derivatives in Euler's equation we obtain

$$\frac{n(y) x'}{\sqrt{1 + x'^2}} = \text{Cte.} \quad (17)$$

If we call  $y_0$  the minimum height from the ground that a ray of light coming from some object reaches before continuing its upward journey, and setting  $x = 0$  there, the condition  $x'(y_0) \rightarrow \infty$  is fulfilled. Then

$$\lim_{y \rightarrow y_0} \frac{n(y)}{\sqrt{\left(\frac{1}{x'}\right)^2 + 1}} = n(y_0), \quad (18)$$

and

$$\frac{n(y) x'}{\sqrt{1 + x'^2}} = n(y_0). \quad (19)$$

Squaring and rearranging the terms,

$$\frac{dx}{dy} = \frac{n(y_0)}{\sqrt{n^2(y) - n^2(y_0)}}. \quad (20)$$

We assume a refractive index profile as the one expressed by Eq. (12) and use it to re-write the expression under the square root. In doing that we take into account that, for air temperature and pressure values near the ground such as those discussed in the previous section,  $n$  ranges from 1.000274, for  $T = 20^\circ$ , to 1.000234, for  $T = 70^\circ$ . So, from  $\alpha = 1 - n_0/n_f$  it is straightforward to infer that the order of magnitude of  $\alpha$  is  $10^{-5}$  and we can neglect, then, terms containing  $\alpha^2$  to obtain

$$\frac{dx}{dy} = \frac{n_f \left(1 - \alpha \exp\left(-\frac{y\alpha}{\beta}\right)\right)}{n_f \sqrt{2\alpha} \exp\left(-\frac{y_0\alpha}{2\beta}\right) \sqrt{1 - \exp\left(-\frac{y-y_0}{\beta}\right)}}. \quad (21)$$

Integrating between 0 and  $x$  and between  $y_0$  and  $y$  we get

$$x = \gamma \int_{y_0}^y \frac{dy}{\sqrt{1 - \exp\left(-\frac{y-y_0}{\beta}\right)}}, \quad \text{with} \quad (22)$$

$$\gamma = \frac{1 - \alpha \exp\left(-\frac{y_0}{\beta}\right)}{\sqrt{2\alpha} \exp\left(-\frac{y_0}{2\beta}\right)}.$$

Solving the integral, we have finally been able to infer the expression defining the path of the light rays in the first quadrant of  $x - y$  plane as

$$x = 2\beta\gamma \ln \left( 1 + \sqrt{1 - \exp\left(-\frac{y-y_0}{\beta}\right)} \right) + \gamma(y-y_0). \quad (23)$$

For negative  $x$  values Eq. (23) defines the light path in the second quadrant, just the mirror image of the one obtained for the first.

### 3.2. Description and analysis.

Light rays leaving a point object start its way towards the ground following different directions. Some rays reach the ground being absorbed by it. Others are refracted upward before reaching the ground. Whether one thing or the other happens depends on the angle that the ray coming from the object makes with the ground, which is assumed to be horizontal. There is a limiting angle, which we will call  $\theta$ , for which the ray will barely touch the ground before continuing its way up. If the rays leave the object forming angles larger than  $\theta$  with the ground, they will be absorbed by the ground, otherwise the rays will bend upward before reaching it. The distance from the object at which a ray hits the ground or reaches its minimum height also depends on that angle. This

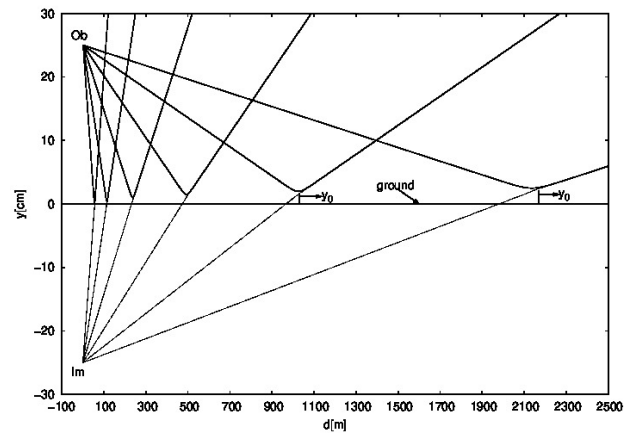


FIGURE 4. Light ray paths. The height from the ground is displayed as a function of the distance to the object for some rays. The object point from which the light comes and its virtual image are also shown.

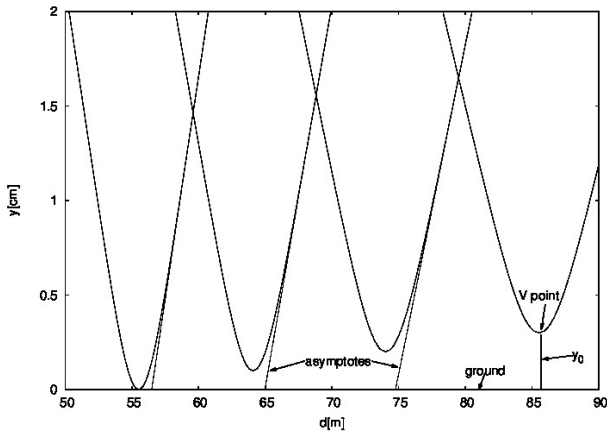


FIGURE 5. Light ray paths close to V points. Enlarged image of some light rays around V points (see text) and their asymptotes are shown.

behavior of the rays is illustrated in Fig. 4, where the height from the ground,  $y$ , as a function of the distance to the object,  $d$ , is displayed.

Figure 4 was drawn up by means of Eq. (23), adopting  $\alpha = 1.10865 \times 10^{-5}$  and  $\beta = 0.33$ , the values that we used in Sec. 2 to fit our calculations. We should note that Eq. (23) was achieved by setting  $x = 0$  at  $y = y_0$  for each ray. Then, in order to refer everything to the same point, we have calculated the shift of every ray with respect to each other by imposing that they all pass through the same point object. So, to be clear:  $x$  is 0 at the point of closest approach to the ground of each ray;  $d$  is 0 at the point object. The virtual image of a hypothetical point object located 25 cm above the ground is also shown in the figure.

Figure 5 shows an enlarged image of some light paths, just to observe their behavior around the point  $(0, y_0)$ , which will be called “V point” from now on. Straight dashed lines represent the asymptotic approach of the light ray paths. These straight lines are given by the equation

$$y = \frac{1}{\gamma}x - \beta \ln 4 + y_0, \quad (24)$$

which is easily obtained from Eq. (23) taking into account that the exponential tends to 0 when  $y$  takes very large values. As can be seen from the figure, the curves representing the light ray paths approach very quickly to their asymptotes as we move away from V point, being confused with them a few millimeters further.

Before we go any further, we take advantage of Eq. (24) to obtain an expression for the limiting angle, which we referred to above, that allows to distinguish the light rays absorbed by the ground from those refracted upwards. The angle that the ray coming from the object makes with the ground is just the angle that its asymptote makes. So, to find the limiting angle we simply have to find the slope of the asymptote to the ray that barely touch the ground for which  $y_0 = 0$ . Then, by setting  $y_0 = 0$  in Eq. (24), and taking into account that  $\alpha \ll 1$ ,  $\theta$  is obtained as

$$\theta = \arctan(\sqrt{2\alpha}) \quad (25)$$

From Figs. 4 and 5 it appears that the light paths through the atmosphere given by Eq. (23) are practically straight lines from the object to very close to the point where they are bent upward to eventually reach the observer’s eyes. In other words, inferior mirages like the ones we are studying in the present article are due to what happens around V points.

Equation (23), in addition to the description of the light ray’s path, is a source of much relevant information. We will use it below to learn about the height from the ground at which the right conditions for an inferior mirage to occur are met. Since everything happens around V points, we could get our objective by estimating the  $y_0$  values of the rays that could reach the observer’s eyes. In order to do that, letting  $y_0$  vary in Eq. (23) we have calculated  $x$  for picked  $y$  values. The  $y$  values we have chosen to do the calculations, which will be called  $y_{ob}$  hereafter, are some feasible values of the height from the ground at which the observer’s eyes could be. To draw Fig. 6, the calculated  $x$  values have then been referred to a hypothetical object point located at  $h = 1$  m from the ground.

Each point of a given curve in Fig. 6 represents the  $y_0$  value of the ray that reaches the observer’s eyes located at the height  $y_{ob}$  from the ground and at the distance  $d$  from the object. In Fig. 7, the  $y_0$  value is shown as a function of the distance to the object for different values of  $h$ , assuming the observer’s eyes 1 m above the ground.

From Figs. 6 and 7 it is clear that rays with different  $y_0$  values will reach the observer’s eyes depending on the distance to the object, which was varied between a minimum and a maximum value. On the one hand, there is a minimum

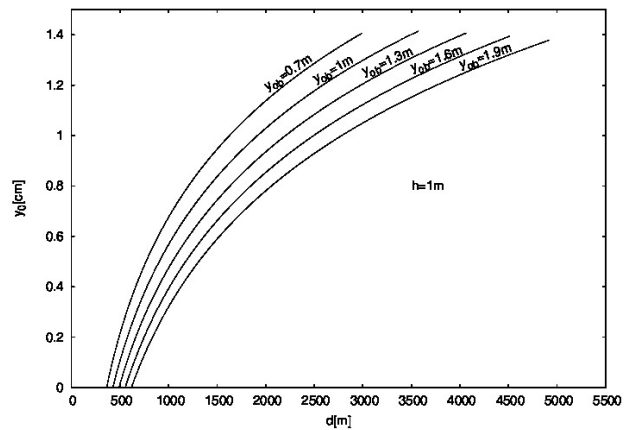


FIGURE 6. Light rays from a point object reaching the observer’s eyes. The  $y_0$  value of the ray reaching the observer’s eyes, who is at the distance  $d$  from the object, is shown for different  $y_{ob}$  values. The point object was assumed to be at  $h = 1$  m above the ground.

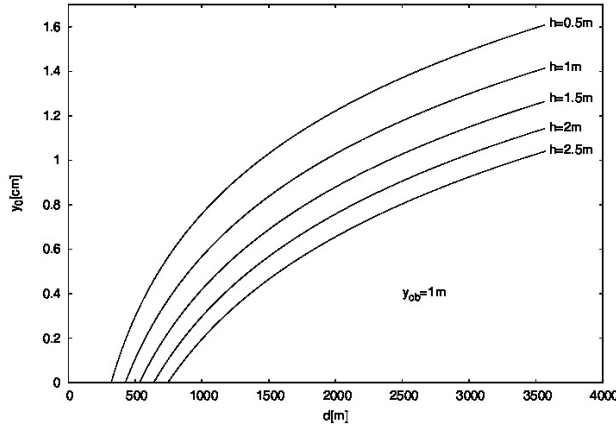


FIGURE 7. Light rays from different point objects reaching the observer's eyes. The  $y_0$  value of the ray reaching the observer's eyes, who is at the distance  $d$  from the object, is shown for different  $h$  values. The observer's eyes were assumed to be at  $y_{ob} = 1$  m above the ground.

distance to the object,  $d_{\min}$ , that the observer should be to witness a mirage, which can be calculated as

$$d_{\min} = \frac{h + y_{ob}}{\tan \theta} = \frac{h + y_{ob}}{\sqrt{2\alpha}}. \quad (26)$$

Given that  $\alpha$  can be obtained from Eq. (12), as we pointed out in Sec. 2, and taking into account the dependence of the refractive index on the temperature,  $d_{\min}$  can be written in terms of the surface and the environment temperatures. So, writing  $\alpha$  in terms of  $n_0$  and  $n_f$ , and taking into account Eqs. (7) and (9). Equation (26) can be written as a function of the surface and the environment temperatures as

$$d_{\min} = \frac{h + y_{ob}}{\sqrt{\frac{2A(T_0 - T_f)}{T_0(T_f + A)}}}, \quad (27)$$

where  $A = \delta \times 10^{-6} 273$ .

Taking into account the range of variability of the parameters, we can easily do some calculations. The observer, whose eyes are 1m from the ground, should be at a distance greater than 671 m from a 5 m high palm tree to see the image of its tip, and at a distance greater than 113m to see its base. Those values will change to 1280 and 215 m, respectively, for the smallest  $\alpha$  values.

On the other hand, and just to impose an upper limit on how far the observer could be to see a mirage, the calculated distance was constrained to be smaller than the distance to the horizon for the adopted  $y_{ob}$  value. The ray with the maximum  $y_0$  value that the observers will be able to see is that reaching their eyes when they are located at the distance of the horizon from the object. This maximum  $y_0$  value, called  $y_0^m$  from now on, is plotted in Fig. 8 as a function of  $y_{ob}$  for different  $h$  values.

In typical situations of sighting of this type of mirages, walking or driving along a paved road, the observer's eyes are not closer to the ground than 1 m. It is apparent from

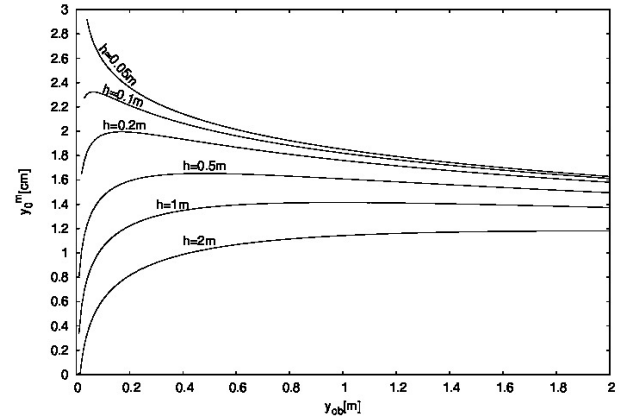


FIGURE 8. Light rays with the maximum  $y_0$  value reaching the observer's eyes.  $y_0^m$  is displayed as a function of  $y_{ob}$  for point objects located at different height,  $h$ , above the ground.

Figs. 6, 7, and 8 that, for the adopted  $\alpha$  and  $\beta$  values, the rays that could reach the observer's eyes are those characterized with  $y_0$  values smaller than 2 cm. Actually, we can say that rays with  $y_0$  so large hardly reach the observer's eyes, since these maximum values are reached for very long distances to the object. Rarely is the ground surface flat and unobstructed to allow the observer to simultaneously view the object and its image at such great distances.

For different  $\alpha$  and  $\beta$  values, that is, for different temperature profiles, obtained by varying  $T_f$ ,  $T_0$ , and  $Q$ , as explained in Sec. 2,  $y_0^m$  may reach at the most 5.5 cm for  $y_{ob} = 1$  m. This value is an upper limit which means that, regardless of the distance from the object, observers whose eyes were 1 m from the ground would not be able to see a mirage, if it occurred at a greater than 5.5 cm height, that is, if all the light rays coming from the object are bent upward in air layers higher than 5.5 cm. In any case, this type of mirages is the result of what happens a few centimeters from the ground, the layer of air that meteorologists call "the microlayer".

#### 4. Summary and conclusions

In this article we have found a simple analytic expression that describes the path of light rays in a vertical plane on the occasion of a inferior mirage, for an assumed refractive index profile.

Using Cartesian coordinates, we have assumed that the geometrical optics laws apply and have taken advantage of the Fermat's principle to reach that expression.

A simple and approximate modeling of the microlayer has allowed us to justify, in Sec. 2, the expression  $n(y) = n_f[1 - \alpha \exp(-y/\beta)]$  assumed to represent the atmospheric refractive index. Many authors have suggested a temperature profile, on which the refractive index depends, such as that obtained from our simple model.

Some articles on the subject propose, for some particular  $n$  profiles, analytic solutions to represent the light ray paths. Even for a refractive index profile similar to the one

we have used, approximate expressions are found in the literature. However, as far as we know, no analytic solution as simple as ours has been proposed. Focusing on inferior mirages only, rather than image formation in general, is what has allowed us to make particular considerations that simplify the problem and allow us to achieve such a simple expression. Having such a simple analytic expression allows to obtain a lot of valuable information, in addition to simply knowing the ray paths. We only need to know the temperature profile in the microlayer. Empirical data of the ground temperature and the amount of heat emitted from the soil in sunny days, when a mirage may take place, have allowed us to adjust the ranges of variability of the parameters involved in the model, as we mentioned in Sec. 2.. In this way, we were able to set, for example, limits on the thickness of the atmospheric layer where

the mirages usually seen on roads occur. Empirical temperature data also allow us to estimate the minimum distance at which the images can be seen, since we were able to express it in terms of air temperature.

We plan to continue working in this line related to optical phenomena in plasmas and gases such as planetary or stellar atmospheres. In particular, in a future work we intend to study superior mirages quite frequently seen in cold regions.

## Acknowledgments

Thanks are due to Santiago Hurtado, teacher at the Facultad de Ciencias Astronómicas y Geofísicas, for valuable suggestions and discussions.

- 
1. A. Danjon, *Astronomie generale. Astronomie spherique et elements de mecanique celeste*, 2nd ed., (J. & R. Sennac editeurs, Paris, 1959) pp. 143.
  2. A. I. Mahan, Astronomical refraction, some history and theories, *Appl. Opt.* **1** (1962) 497. <https://doi.org/10.1086/110225g.1364/AO.1.000497>.
  3. B. Garfinkel, Astronomical refraction in a polytropic atmosphere, *Astron. J.* **72** (1967) 235, <https://doi.org/10.1086/110225>.
  4. A. Yu. Yatsenko, Exact theory of astronomical refraction for the real atmosphere, *A&AS* **111** (1995) 579.
  5. A. T. Young, Understanding astronomical refraction, *The Observatory* **126** (2006) 82.
  6. T. Corbard, R. Ikhlef, F. Morand, M. Meftah, C. Renaud, On the importance of astronomical refraction for modern solar astrometric measurements, *MNRAS* **483** (2019) 3865. <https://doi.org/10.1093/mnras/sty3391>.
  7. J. Evans, M. Rosenquist,  $F = ma$  optics, *Am. J. Phys.* **54** (1985) 876. <https://doi.org/10.1119/1.14861>.
  8. J. Evans, Simple forms for equations of rays in gradient-index lenses, *Am. J. Phys.* **58** (1980) 773. <https://doi.org/10.1119/1.16357>
  9. B. D. Nener, N. Fowkes, and L. Borredon, Analytical models of optical refraction in the troposphere, *J. Opt. Soc. Am. A.* **20** (2003) 867. <https://doi.org/10.1364/JOSAA.20.000867>.
  10. N. Fowkes and B. D. Nener, Microwave propagation over the Earth: image inversion, *Journal of Engineering Mathematics* **53** (2005) 253. <https://doi.org/10.1007/s10665-005-9015-0>.
  11. M. Berger, T. Trout, and N. Levit, Ray Tracing Mirages, *IEEE Computer Graphics and Applications* **10** (1990) 36. <https://doi.org/10.1109/38.55151>.
  12. F. K. Musgrave, A Note on Ray Tracing Mirages, *IEEE Computer Graphics and Applications* **10** (1990) 10. <https://doi.org/10.1109/38.62692>.
  13. J. Stam, E. Languenou, Ray Tracing in Non-Constant Media, *In Proc. Eurographics Workshop on Rendering* (1996) 225. <https://doi.org/10.1007/978-3-7091-7484-5-23>.
  14. D. Gutierrez, F. J. Seron, A. Munoz and O. Anson, Simulation of atmospheric phenomena, *Computers & Graphics* **30** (2006) 994. <https://doi.org/10.1016/j.cag.2006.05.002>.
  15. M. Born, and E. Wolf, *Principles of Optics*, (Pergamon Pres 1959).
  16. J. D. Jackson, *Classical Electrodynamics*, (Wiley, New York 1975).
  17. R. Stull, An Introduction to Boundary Layer Meteorology. Kluwer Academic Publishers. Dordrecht. The Netherlands (1988).
  18. W. G. Kannuliuk, and E. H. Carman, The Temperature Dependence of the Thermal Conductivity of Air, *Australian J. Sci. Res.* **4** (1951) 305. <https://doi.org/10.1071/CH9510305>.
  19. P. E. Ciddor, Refractive index of air: new equations for the visible and near infrared, *Applied Optics* **35** (1996) 1566. <https://doi.org/10.1364/AO.35.001566>.
  20. J. R. Garrat, Extreme Maximum Land Surface Temperatures, *Journal of Applied Meteorology* **31** (1991) 1096. [https://doi.org/10.1175/1520-0450\(1992\)031\(1096:EMLST\)2.0.CO;2](https://doi.org/10.1175/1520-0450(1992)031(1096:EMLST)2.0.CO;2).
  21. B. G. Heusinkveld, On dew and micrometeorology in an arid coastal ecosystem, (Wageningen University and Research, 2008).
  22. M. Pfeiffer *et al.*, Soil Temperature and Relative Humidity at the Yungay Hiperarid site, Atacama Desert, Chile 2015-2017. PANGAEA, Data Publisher for Earth & Environmental Science (2021). <https://doi.pangaea.de/10.1594/PANGAEA.929564>.